Received June 2, 2020, accepted June 11, 2020, date of publication June 16, 2020, date of current version June 30, 2020.

Digital Object Identifier 10.1109/ACCESS.2020.3002759

A New LLSC Series Quasi-Resonant Converter With Narrow Switching Frequency Variation

TIANYU ZHU[1], YANCHAO JI[1], (Member, IEEE), JIANZE WANG[1], AND YIQI LIU[2]
[1]Harbin Institute of Technology, Harbin 150001, China
[2]Northeast Forestry University, Harbin 150040, China

Corresponding author: Yiqi Liu (ee_617@nefu.edu.cn)

ABSTRACT In this paper, the FHA model including the stray capacitance is analysed. The causes of the voltage gain distortion are studied. Limiting the working frequency is an effective method to solve the voltage gain distortion problem. A new type of the LLSC converter is proposed in the paper. It can regulate the voltage at a constant frequency. At the same time, the soft switch can be realized if the parameter design is reasonable. The proposed converter can overcome the voltage gain distortion problem and obtain the high efficiency at the light load condition. Some mathematical analyses are used to prove that the proposed converter can avoid the voltage gain distortion problems. The simulation and experimental results based on a 200W LLSC converter prototype confirm the correctness of the topology.

INDEX TERMS Constant-frequency voltage regulation, soft switching, voltage gain distortion, high efficiency.

NOMENCLATURE

Symbol	Quantity
C_{eq}	Equivalent capacitance
C	Basic capacitance
a	phase shift
M	Voltage gain
f_r	Resonant frequency
f_s	Switching frequency
k	Inductance ratio
Q	Quality factor
L_r	Resonant inductance
L_m	Transformer inductance
C_r	Resonant capacitance
C_s	Stray capacitance
R_{ac}	Equivalent AC load
I_{Lr}	Resonant current
I_{byp}	Bypass current
P_t	Apparent power
K_g	Magnetic core geometric
K_f	Waveform factor
B_{AC}	Window factor

The associate editor coordinating the review of this manuscript and approving it for publication was Jonghoon Kim.

I. INTRODUCTION

Nowadays the LLC (inductor-inductor-capacitor) resonant converter shown in Fig. 1 is employed in numerous applications including photovoltaic systems, such as energy storage system, electric vehicle charging system, and so on [1]–[4]. Compared with the non-isolated converter, the advantages of the LCC resonant converter with high efficiency are summarized as follows: ZVS (Zero Voltage Switching) is realized for the primary-side MOSFETs and ZCS (Zero Current Switching) is realized for the secondary-side rectifier diodes [5], [6]. Some problems appear in this new application. In the photovoltaic systems and the electric vehicle charging applications, the voltage gain distortion problem has received more and more attention. As a traditional LLC converter, the voltage gain decreases with the increase of switching frequency in the buck mode. In fact, the voltage gain decreases and then increases with the increase of switching frequency in the buck mode that is called the voltage gain distortion.

Some complex resonant converters are used to solve the problem of voltage gain distortion and improve the light-load stability, such as the LCC (inductor-capacitor-capacitor) converters and the LCLC (inductor-capacitor-inductor-capacitor) converters [7]–[10]. Although the LCC converter has better load-adjustment characteristics than the LLC converter, it has the disadvantages of complex parameter design and variable

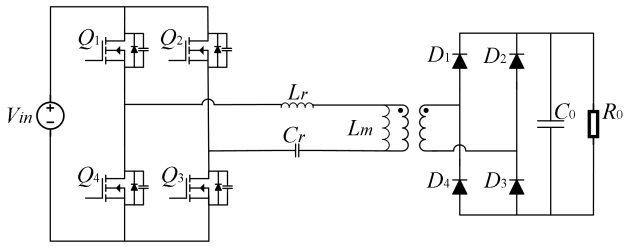

FIGURE 1. Conventional isolated LLC resonant converter.

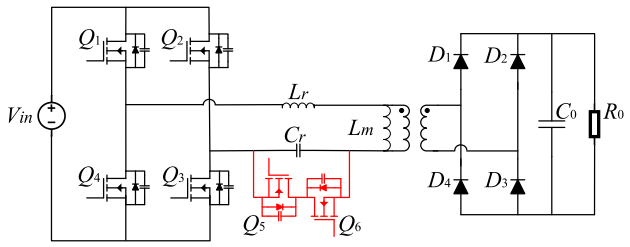

FIGURE 2. The proposed LLSC converter.

switching frequency. Also, the LCC converters lose ZVS under the light-load condition, and then the converter's losses are increased. The LCLC converter add more resonance elements. Most importantly, the additional resonance elements make the transfer function of the system produce new poles. The effect of these new poles on the complexity of the control system is identical to the voltage gain distortion problem under the light-load condition.

In [11], some analyses of the light-load regulation are made through impedance asymptote. An additional capacitor is added in parallel with L_r. In [12], an intermittent control method is introduced to increase the equivalent load in light-load condition which increases the complexity of control system.

The above research focuses on solving the voltage gain distortion problem, instead of finding the cause of the problem. In general, the fundamental harmonic approximation (FHA) model is suitable for analysing the output voltage of the ideal LLC resonant converter that works under light-load conditions [11], [13]–[18]. For the actual LLC converter, the junction capacitor of the secondary-side rectifier diodes and the stray capacitance of the transformer consists of the stray capacitance of the converter [19]–[21]. Meanwhile, the stray capacitance induces an additional extreme point that causes the voltage gain distortion under the light-load condition [11], [17]–[23].

In this paper, the FHA model including the stray capacitance is analysed. The causes of the voltage gain distortion are studied. Limiting the working frequency is an effective method to solve the voltage gain distortion problem. The constant-frequency LLSC quasi-resonant converter is proposed to solve the voltage gain distortion under the light-load condition. The primary-side resonant capacitor is parallelly connected with a set of reverse series MOSFETs. The primary-side equivalent capacitance is adjusted by controlling the turn-on and turn-off of the MOSFETs. Therefore, the output voltage can be adjusted at the constant frequency. Furthermore, the proposed converter has better overall efficiency and power density.

The rest sections of this paper are organized as follows: Section 2 analyses the operating principle of the proposed converter; Section 3 analyses the voltage gain of the proposed converter; Section 4 discusses the cause of the light-load problem; Section 5 analyses the proposed converter through experimental results. Finally, the conclusions are drawn in Section 6.

II. THE PROPOSED LLSC CONVERTER AND ITS OPERATIONAL PRINCIPLE

Fig. 2 depicts an improved LLSC converter structurally different from the LLC converter. For the improved LLSC converter, a resonant capacitor is combined with a set of anti-series MOSFETs to form a SCC (switch controlled capacitor) module. The frequency of the bypass MOSFET is identical to the frequency of the MOSFET which makes up the converter's primary side, and there is a certain phase shift between Q_1 and Q_5. The shift decides the bypass period of the resonant capacitor. The output voltage can be changed adjusting the phase shift between Q_1 and Q_5.

The LLSC converter's operational principle is identical to the operational principle of the LLC converter. Dead time is the first period in switching cycle shown in Fig. 3 (t_0-t_1). The second period is a resonant state. In this state, the resonant inductor, excitation inductor and resonant capacitor shown in Fig.3 participate in resonance (t_1-t_3). Specially, the exit of resonant capacitor should be noticed shown in Fig. 3 (t_3-t_4). The resonant cavity only has two inductors in some periods, so the LLSC converter is called the quasi-resonant converter.

In this paper, the effect of parasitic parameters is mainly discussed. Detailed analysis of the LLSC converter's operational principle can be found in [24].

III. VOLTAGE GAIN MODEL OF LLSC CONVERTER

The improved converter is also a resonant converter, so the FHA model of the LLC converter can be used to analyse the voltage gain.

A. THE RELATIONSHIP BETWEEN THE EQUIVALENT CAPACITANCE AND THE DRIVER DELAY

The SC structure was first proposed in [25]. The principle of the work is not described in detail in this article. The working state of the SCC can be divided into two categories: full wave and half wave. Because SC is used as a resonant capacitor, the full wave SCC structure is used in this paper.

The equivalent capacitance of a full wave SCC is derived as follows and shown in Fig. 5.

$$\frac{C_{eq}}{C} = \frac{1}{2 - (2\alpha - \sin 2\alpha)/\pi} \tag{1}$$

where C_e is the equivalent capacitance and C is the basic capacitance.

There are two linear regions (I, III) and one non-linear regions (II) to be chosen. The first gain range of the equivalent

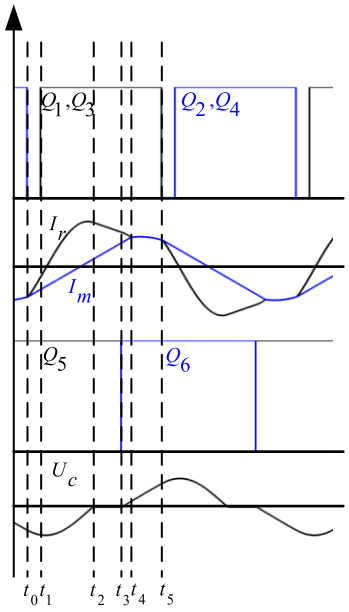

(a)

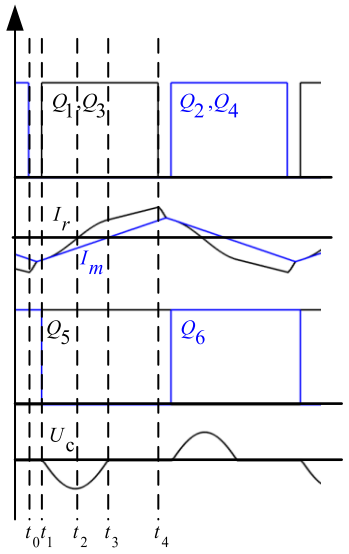

(b)

FIGURE 3. Commutation process of the LLSC converter (a)Boost mode (b)Buck mode.

capacitance is narrow (0,3) and its rate of change is slow. The second region (II) has a wider gain range (3,20) and moderate rate. The last region has the widest gain range (0, $+\infty$) but the rate of change is so quick that there are potential risks in the control system. The FHA model should be analysed before deciding the working region.

B. THE VOLTAGE GAIN MODEL BY THE FUNDAMENTAL WAVE ANALYSIS

The fundamental harmonic analysis (FHA) model can be used to analyse the voltage gain of the proposed converter.

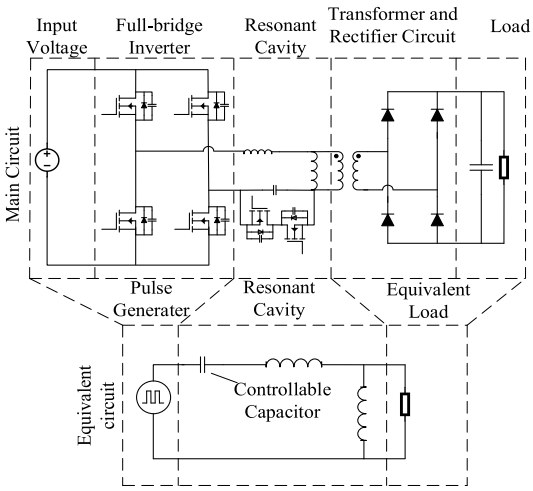

FIGURE 4. Equivalent circuit diagram of the LLSC converter.

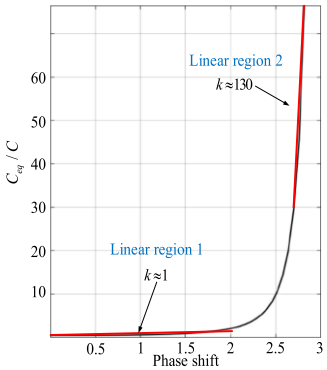

FIGURE 5. Relationship between the equivalent capacitance and the phase shift between Q_1 and Q_5.

TABLE 1. Resonant parameters.

Parameters	LLSC	LLC
Resonant inductance	50μH	50μH
Resonant capacitor	10nF	50nF
Magnetic inductance	100μH	100μH
Transformer ratio	2:1	2:1

Different from the LLC converter, there are two methods of changing the operating frequency of the converter and the driver delay. The FHA model of the improved converter can be organized into the following form

$$M = \frac{1}{\sqrt{\left(1 + \frac{1}{k} - \frac{k}{\lambda^2}\right) + \frac{L_r}{C_r}\frac{1}{R_1^2}\left(\lambda - \frac{1}{\lambda}\right)^2}} \tag{2}$$

where $\lambda = f_s/f_r$, $k = L_m/L_r$

Two sets of converter parameters are designed in Table 1 and shown to plot the gain curves.

Fig. 6 shows the voltage gain factor of the designed LLC converter. According to Eq.(3), a 3D surface can be obtained shown in Fig. 7, which describes the voltage gain through the change of C_r and f_s. Especially, the proposed converter can regulate the voltage through changing the equivalent capacitance shown in Fig. 8.

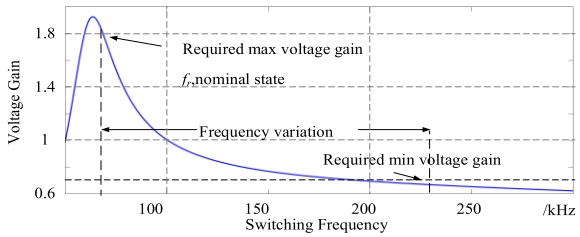

FIGURE 6. LLC converter voltage gain according to FHA model.

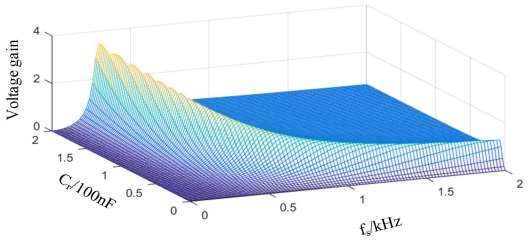

FIGURE 7. LLSC converter's voltage gain curve in 3D.

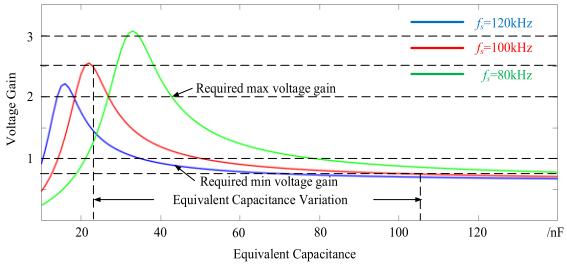

FIGURE 8. LLSC converter's voltage gain according to FHA model.

As shown Fig. 8, the voltage gain changes faster between 10-150nF. The region I is too narrow to meet the requirement. The region III can meet the requirement but it is difficult to control. The region II is an appropriate region which has appropriate range and speed of change.

Compared with Fig. 8, the proposed converter can offer larger voltage regulation range. In the boost mode, the resonant capacitance and switching frequency decide the max voltage gain. The proposed converter can obtain higher voltage gain through increasing the equivalent capacitance instead of decreasing the frequency. This is beneficial to improving the power density of the converter. On the other hand, the proposed converter can obtain higher voltage gain through increasing the equivalent capacitance and decreasing the frequency at the same time.

IV. THE VOLTAGE GAIN DISTORTION PROBLEM

At the light loads, the voltage gain distortion is a serious problem for the conventional LLC converters. This problem occurs in the Buck mode under the light load condition. When the operating frequency of the system is high, the output voltage increases as the operating frequency increases. This phenomenon is called voltage gain distortion and mainly caused by the stray capacitance in the circuit. To better explain this phenomenon, it is necessary to establish an FHA model including the stray capacitance parameters.

C_s (stray capacitance) of the LLC converter consists of three parts: the rectifier diode junction capacitance, the transformer, and the output filter capacitor. After converting the stray capacitance parameters to the primary side, the circuit can be simplified into the following form.

The voltage gain FHA model considering the stray capacitance can be expressed by the following Eq. (3).

$$H(s) = \frac{sL_m // R_{ac} // \frac{1}{sC_s}}{\frac{1}{sC_r} + sL_r + sL_m // R_{ac} // \frac{1}{sC_s}} \tag{3}$$

Equation (3) can be simplified as follows

$$M = \frac{k\lambda^2}{\sqrt{\left[\left(1-\lambda^2\right)\left(k\alpha\lambda^2-1\right)+k\lambda^2\right]^2+\left[\lambda kQ\left(\lambda^2-1\right)\right]^2}} \tag{4}$$

where $\lambda = f_s/f_r, \alpha = C_s/C_r, k = L_m/L_r$

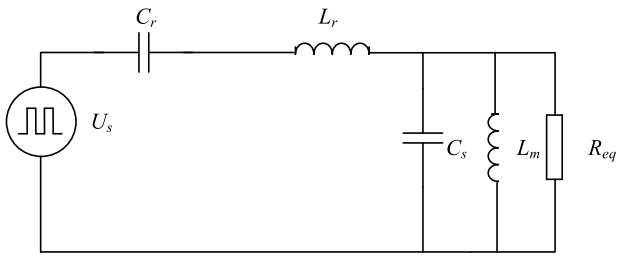

FIGURE 9. Equivalent circuit diagram of the LLC converter considering C_s.

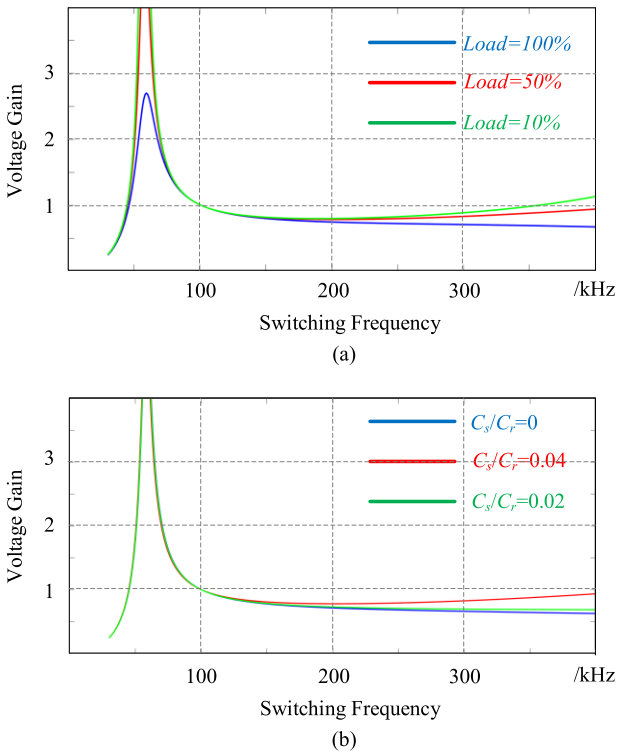

FIGURE 10. Voltage gain curve by Eq.(5) LLC converter (a)different load (b)different C_s/C_r.

Figure. 10 depicts Eq.(4) with different parameters. With the load reducing, the voltage gain distortion appears and

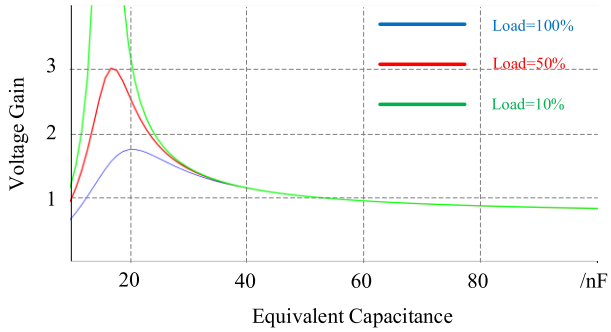

FIGURE 11. Voltage gain curve by Eq. 5 with different loas forthe LLSC converter.

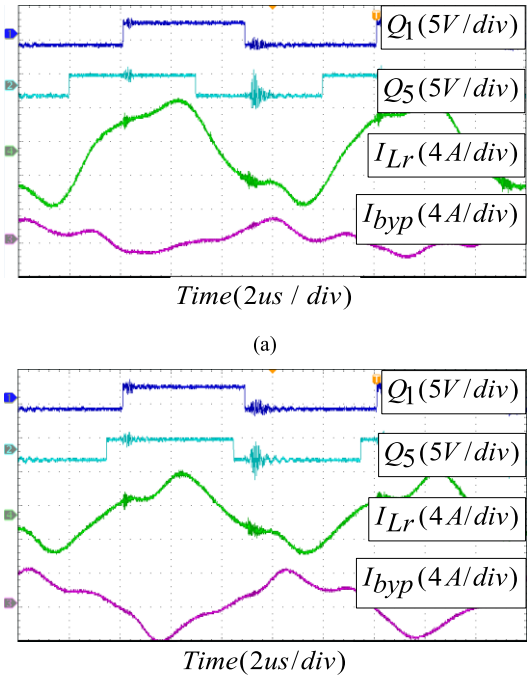

FIGURE 12. Experimental waveforms(a)full load (b)light load.

TABLE 2. Experiment parameters.

Parameters	LLSC	LLC
Input voltage	200V	200V
Output voltage	75-250V	75-190V
Resonant inductance	50μH	50μH
Resonant capacitor	10nF	50nF
Magnetic inductance	100μH	100μH
Transformer ratio	2:1	2:1
Operating Frequency	100kHz	50-250kHz
Rating Load	40Ω	40Ω

increases with the increase in stray capacitance. To better analyse the causes of the voltage gain distortion, the poles of FHA models with the stray capacitors are analysed. The pole of Eq. (3) can be found through Eq. (5).

$$\sqrt{\left(1+\frac{1}{k}-\frac{k}{\lambda^2}\right)+\frac{L_r}{C_r}\frac{1}{R_1^2}\left(\lambda-\frac{1}{\lambda}\right)^2}=0 \qquad (5)$$

TABLE 3. Experiment parameters.

Input voltage	200V	Load	40Ω
Components	Notation	LLSC	LLC
Main transformer	Core	PQ26/25	PQ32/30
	$N_p:N_s$	76:38	86:43
	L_m	100μH	100μH
Resonant components	C_r	20nF,Non-inductive capacitor	50nF,Non-inductive capacitor
	L_r	50uH,CH172125	50uH,CH172125
Primary switches	Q_1~$Q6$	FQA30N40	FQA30N40
Secondary diodes	D_1~D_4	MUR3040	MUR3040

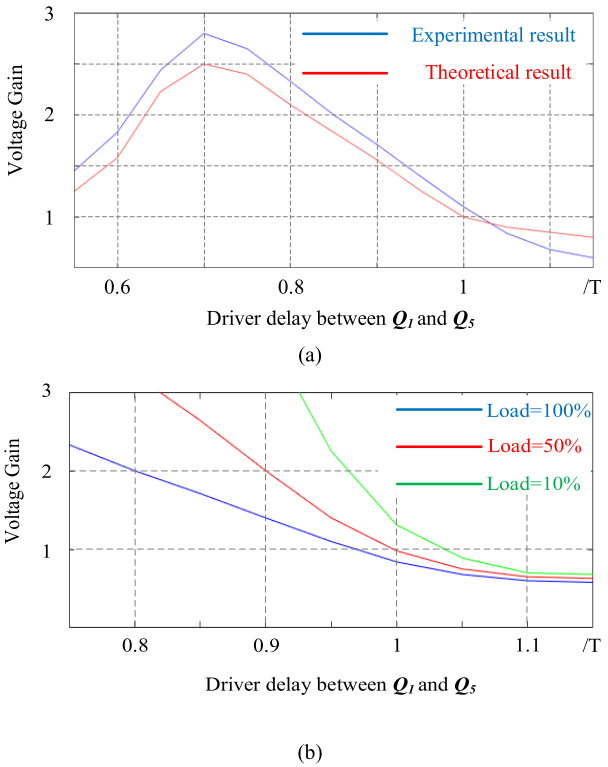

FIGURE 13. LLSC converter voltage gain experiment curve at 100kHz (a)full load (b)light load.

Simplify

$$a_1\lambda^4+b_1\lambda^3+c_1\lambda^2+d_1\lambda+e_1=0 \qquad (6)$$

where $a_1=\frac{L_r}{C_rR_1^2}$, $b_1=0$, $c_1=1+\frac{1}{k}-\frac{2L_r}{C_rR_1^2}$, $d_1=0$, $e_1=1-k$

According to the root formula of the quaternary equation of one variable, there is no real root in Eq. (6). Thus there is no poles in the working frequency range in Eq. (2). Therefore the poles are not the cause of the maximum gain. The denominator of Eq. (5) is analysed by derivation, and when the denominator of Eq. (2) has a minimum value, the voltage gain of the converter is the largest.

The denominator of Eq. (4) is

$$\sqrt{\left[\left(1-\lambda^2\right)\left(k\alpha\lambda^2-1\right)+k\lambda^2\right]^2+\left[\lambda kQ\left(\lambda^2-1\right)\right]^2} \qquad (7)$$

There is no zero point in Eq. (7). Similar to Eq. (5), extreme points should be considered.

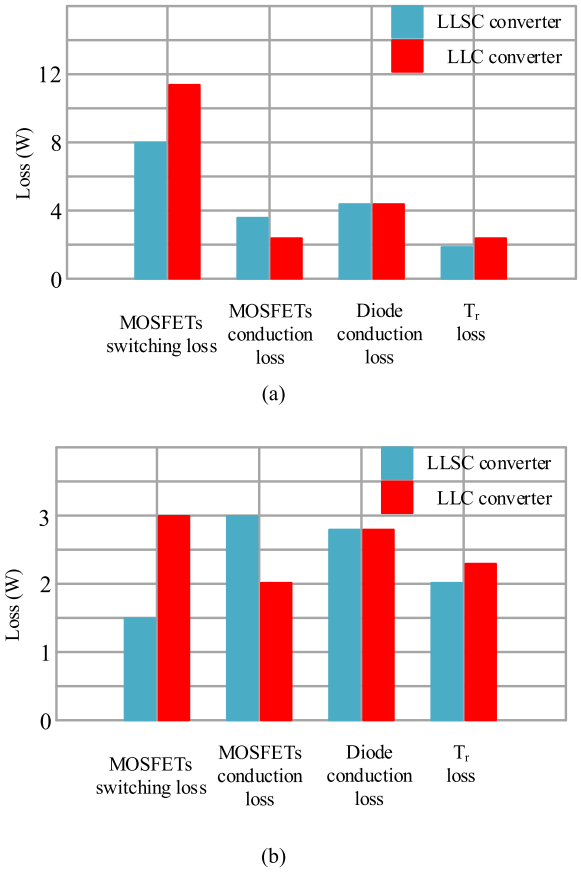

FIGURE 14. Loss comparison experiment between LLSC converter and LLC converter. (a)40Ω Load,output voltage 250V (b) 80Ω Load,output voltage 50V.

Eq. (7) is arranged in the following Eq. (8), (9) and (10)

$$\left[A(\lambda)f\left(\lambda^2\right)+k\right]^2+\left[B(\lambda)f\left(\lambda^2\right)\right]^2 \tag{8}$$

$$A(\lambda)f\left(\lambda^2\right)+k \tag{9}$$

$$B(\lambda)f\left(\lambda^2\right) \tag{10}$$

where $A(\lambda)=1-k\alpha\lambda^2+k$, $B(\lambda)=\lambda kQ$,

$$f\left(\lambda^2\right)=\lambda^2-1$$

Eq. (10) monotonously increases when $\lambda > 1$. The necessary and insufficient condition for the existence of extreme points in Eq. (8) is that the derivative of Eq. (10) is less than zero. Derivation of Eq. (9) can be simplified into

$$\lambda^2 \geq \frac{k\alpha+1+k}{2k\alpha} \tag{11}$$

$$\alpha \geq \frac{1+k}{2k\lambda^2-k} \tag{12}$$

This shows that high operating frequency and large stray capacitance are the necessary conditions for the voltage gain distortion problem. Fig. 11 can prove the above conclusion. Therefore the voltage gain distortion can be eliminated by limiting λ and decreasing α. The proposed converter is a constant frequency converter, where α decreases with the decrease in voltage gain. Therefore the proposed converter can overcome the voltage gain distortion problem.

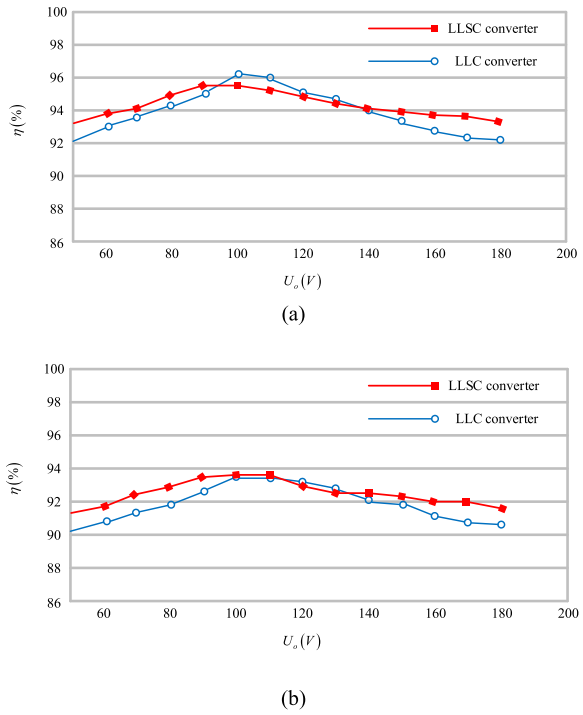

FIGURE 15. Efficiency comparison experiment between LLSC converter and LLC converter. (a)40Ω load. (b)80Ω load.

V. EXPERIMENTAL RESULTS

To prove the theoretical effectiveness of the proposed converter, the LLC converter and proposed converter are built. Figure 12. shows some key waveforms of the proposed converter. The experiment conditions are shown in Table 2. Table 3 shows the component list of the proposed and the LLC converters. The experimental and theoretical gain curves are shown in Fig. 13(a). The FHA model describes the resonant current as sine mode, so there are some differences between the experimental and theoretical results. Fig. 13(b) shows the voltage gain curve at full and light loads. Thus the voltage gain distortion problem can be overcome through regulating the voltage at the constant frequency.

The magnetic core geometric constant method (K_g) is used to design a transformer shown in Eq. (13).The lowest operating frequency of the LLSC converter is higher than the LLC converter's lowest operating frequency so the volume of magnetic element can be reduced.

$$K_g=\frac{P_t}{2\times 0.145K_f^2f^2B_{AC}^2\times 10^{-4}\alpha} \tag{13}$$

where $K_f=4.44$, $B_{AC}=0.05$

The proposed converter's min switching is higher than the LLC converter's. According to Eq. (13), the proposed converter has a smaller Kg, which means the size of the magnetic core can be reduced significantly. Theoretically, the core can be reduced to a quarter of the LLC converter. In practice, it is necessary to consider the actual core.

Fig. 14 discusses the loss of the LLC converter and the proposed converter at different loads. The lower switching current and frequency can reduce the switching loss. The proposed converter has a bigger conduction loss because of the additional MOSFETs. However, it can be significantly reduced through changing the MOSFETs into the MOSFETs which has 0.02Ω conduction resistance. The proposed converter has a smaller transformer which can reduce the iron and copper loss.

Fig. 15 is a comparison between the LLSC converter and the LLC converter in efficiency. In the buck mode, the LLSC converter has a significant advantage. The LLSC converter has a gentle efficiency curve. Thus the LLSC converter is suitable for large range voltage regulation application.

VI. CONCLUSIONS

In this paper, an improved FHA model is analysed. Compared with the traditional FHA model, an additional pole is found which causes the voltage gain distortion under the light-load condition. According to the analysis of this pole, a higher working frequency and the light-load condition are the necessary conditions for the voltage gain distortion. Limiting the maximum working frequency is an effective method to solve the problem under the light-load condition. A new quasi-resonant LLSC converter is proposed, which can regulate the voltage at the constant frequency. Experiments and analyses prove that the proposed converter can adjust output voltage at constant working frequency. Compared with the traditional LLC converter, the proposed has better overall efficiency and larger power density.

REFERENCES

[1] J.-K. Kim, J.-B. Lee, and G.-W. Moon, "Isolated switch-mode current regulator with integrated two boost LED drivers," *IEEE Trans. Ind. Electron.*, vol. 61, no. 9, pp. 4649–4653, Sep. 2014.

[2] I. Demirel and B. Erkmen, "A very low-profile dual output LLC resonant converter for LCD/LED TV applications," *IEEE Trans. Power Electron.*, vol. 29, no. 7, pp. 3514–3524, Jul. 2014.

[3] M. A. Halim, M. N. Hidayat, and M. N. Seroji, "Implementation and analysis of a half-bridge series-parallel LLC loaded resonant DC-DC converter for low power applications," in *Proc. IEEE 10th Int. Conf. Power Electron. Drive Syst. (PEDS)*, Apr. 2013, pp. 634–638.

[4] D.-K. Kim, S. Moon, C.-O. Yeon, and G.-W. Moon, "High-efficiency LLC resonant converter with high voltage gain using an auxiliary LC resonant circuit," *IEEE Trans. Power Electron.*, vol. 31, no. 10, pp. 6901–6909, Oct. 2016.

[5] U. Kundu, K. Yenduri, and P. Sensarma, "Accurate ZVS analysis for magnetic design and efficiency improvement of full-bridge LLC resonant converter," *IEEE Trans. Power Electron.*, vol. 32, no. 3, pp. 1703–1706, Mar. 2017.

[6] H. Li, Z. Zhang, S. Wang, J. Tang, X. Ren, and Q. Chen, "A 300-kHz 6.6-kW SiC bidirectional LLC onboard charger," *IEEE Trans. Ind. Electron.*, vol. 67, no. 2, pp. 1435–1445, Feb. 2020.

[7] X. Liang, *Optimizing the Light Load Performance of LLC Resonant Converter*. Chengdu, China: Univ. Electronic Science and Technology, 2014.

[8] T. B. Soeiro, J. Muhlethaler, J. Linner, P. Ranstad, and J. W. Kolar, "Automated design of a high-power high-frequency LCC resonant converter for electrostatic precipitators," *IEEE Trans. Ind. Electron.*, vol. 60, no. 11, pp. 4805–4819, Nov. 2013.

[9] Z. Li, C.-Y. Park, J.-M. Kwon, and B.-H. Kwon, "High-power-factor single-stage LCC resonant inverter for liquid crystal display backlight," *IEEE Trans. Ind. Electron.*, vol. 58, no. 3, pp. 1008–1015, Mar. 2011.

[10] M. C. Tsai, "A nalysis and implementation of a full-bridge constantfrequency LCC-type parallel resonant converter," *Proc. Inst. Elect. Eng., Electr. Power Appl.*, vol. 141, no. 3, pp. 121–128, May 1994.

[11] C.-O. Yeon, J.-W. Kim, M.-H. Park, I.-O. Lee, and G.-W. Moon, "Improving the light-load regulation capability of LLC series resonant converter using impedance analysis," *IEEE Trans. Power Electron.*, vol. 32, no. 9, pp. 7056–7067, Sep. 2017.

[12] J.-H. Kim, C.-E. Kim, J.-K. Kim, J.-B. Lee, and G.-W. Moon, "Analysis on load adaptive phase-shift control for high efficiency full-bridge LLC resonant converter in light load conditions," *IEEE Trans. Power Electron.*, vol. 31, no. 7, pp. 4942–4955, Jul. 2017.

[13] X. Fang, H. Hu, F. Chen, U. Somani, E. Auadisian, J. Shen, and I. Batarseh, "Efficiency-oriented optimal design of the LLC resonant converter based on peak gain placement," *IEEE Trans. Power Electron.*, vol. 28, no. 5, pp. 2285–2296, May 2013.

[14] Y.-S. Cheng, J.-H. Chen, Y.-H. Liu, K.-L. Huang, and Z.-Z. Yang, "Design of a digitally-controlled LLC resonant converter with synchronous rectification," in *Proc. 1st Int. Future Energy Electron. Conf. (IFEEC)*, Nov. 2013, pp. 772–776.

[15] C. Oeder and T. Duerbaum, "ZVS investigation of llc converters based on FHA assumptions," in *Proc. 28th Annu. IEEE Appl. Power Electron. Conf. Expo. (APEC)*, Mar. 2013, pp. 2643–2648.

[16] S. De Simone, C. Adragna, C. Spini, and G. Gattavari, "Design-oriented steady-state analysis of LLC resonant converters based on FHA," in *Proc. Int. Symp. Power Electron., Electr. Drives, Autom. Motion, SPEEDAM*, May 2006, pp. 200–207.

[17] J.-W. Kim, J.-K. Han, and J.-S. Lai, "APWM adapted half-bridge LLC converter with voltage doubler rectifier for improving light load efficiency," *Electron. Lett.*, vol. 53, no. 5, pp. 339–341, Mar. 2017.

[18] H.-Y. Yoon, H.-S. Lee, S.-H. Ham, H.-J. Choe, and B. Kang, "Off-time control of LLC resonant half-bridge converter to prevent audible noise generation under a light-load condition," *IEEE Trans. Power Electron.*, vol. 33, no. 10, pp. 8808–8817, Oct. 2018.

[19] M. G. L. Roes, J. L. Duarte, and M. A. M. Hendrix, "Disturbance observer-based control of a dual-output LLC converter for solid-state lighting applications," *IEEE Trans. Power Electron.*, vol. 26, no. 7, pp. 2018–2027, Jul. 2011.

[20] J. H. Kim, C.-E. Kim, J.-K. Kim, and G.-W. Moon, "Analysis for *LLC* resonant converter considering parasitic components at very light load condition," in *Proc. 8th Int. Conf. Power Electron. ECCE Asia*, Jun. 2011, pp. 1863–1868.

[21] N. Shafiei, M. Ordonez, M. Craciun, C. Botting, and M. Edington, "Burst mode elimination in high-power resonant battery charger for electric vehicles," *IEEE Trans. Power Electron.*, vol. 31, no. 2, pp. 1173–1188, Mar. 2016.

[22] J. Qin, Z. Moussaoui, J. Liu, and G. Miller, "Light load efficiency enhancement of a LLC resonant converter," in *Proc. 26th Annu. IEEE Appl. Power Electron. Conf. Expo. (APEC)*, Mar. 2011, pp. 1764–1768.

[23] B. Wang, X. Xin, S. Wu, H. Wu, and J. Ying, "Analysis and implementation of LLC burst mode for light load efficiency improvement," in *Proc. 24th Annu. IEEE Appl. Power Electron. Conf. Expo.*, Feb. 2009, pp. 58–64.

[24] D. Czarkowski and M. K. Kazimierczuk, "Phase-controlled series-parallel resonant converter," *IEEE Trans. Power Electron.*, vol. 8, no. 3, pp. 309–319, Jul. 1993.

[25] T. Zhu, Y. Ji, J. Wang, and Y. Liu, "A novel constant-frequency quasi-resonant converter," *IEEE Access*, vol. 6, pp. 39635–39642, 2018.

[26] W.-J. Gu and K. Harada, "A new method to regulate resonant converters," *IEEE Trans. Power Electron.*, vol. PEL-3, no. 4, pp. 430–439, Oct. 1988.

TIANYU ZHU was born in Heilongjiang, China, in 1992. He received the B.S. degree from the School of Electrical Engineering and Automation, Harbin Institute of Technology, Harbin, China, in 2015, where he is currently pursuing the Ph.D. degree in electrical engineering. His current research interests include insulated dc/dc converter and topology.

YANCHAO JI (Member, IEEE) received the B.Eng. and M.Eng. degrees in electrical engineering from Northeast Dianli University, Jilin, China, in 1983 and 1989, respectively, and the Ph.D. degree in electrical engineering from North China Electric Power University, Beijing, China, in 1993. He joined the Department of Electrical Engineering, Harbin Institute of Technology, Harbin, China, in 1993. From 1995 to 1996, he was an Associate Professor with the Department of Electrical Engineering, Harbin Institute of Technology, where he is currently a Professor. His current research interests include pulse width modulation technique, power converter, and flexible ac transmission systems devices.

JIANZE WANG received the B.E., M.E., and Ph.D. degrees in electrical engineering from the Harbin Institute of Technology, Harbin, China, in 1993, 1996, and 1999, respectively. He joined the Harbin Institute of Technology, in 1999, and is currently a Research Professor. From July 2003 to December 2003, he was a Visiting Scholar with Hong Kong Polytechnic University, Hong Kong. His current research interests include power electronics, multilevel converters, and digital signal-processor-based power quality control systems.

YIQI LIU received the B.S. degree in electrical engineering from Northeast Agriculture University, Harbin, China, in 2009, the M.S. degree in electrical engineering from the Tianjin University of Technology, Tianjin, China, in 2012, and the Ph.D. degree in electrical engineering from the Harbin Institute of Technology, Harbin, in 2016. From 2013 to 2015, he was a Visiting Ph.D. Student with the Center for Ultra-Wide-Area Resilient Electric Energy Transmission Networks (CURENT), University of Tennessee, Knoxville, TN, USA, with support from the China Scholarship Council. He joined Northeast Forestry University, Harbin, in 2016, and is currently working as an Associate Professor. His current research interests include power electronics for renewable energy sources, multilevel converters, high-voltage direct-current (HVDC) technology, and microgrid clusters.